

# Signal Enhancement of Silicon Nanowire-Based Biosensor for Detection of Matrix Metalloproteinase-2 Using DNA-Au Nanoparticle Complexes

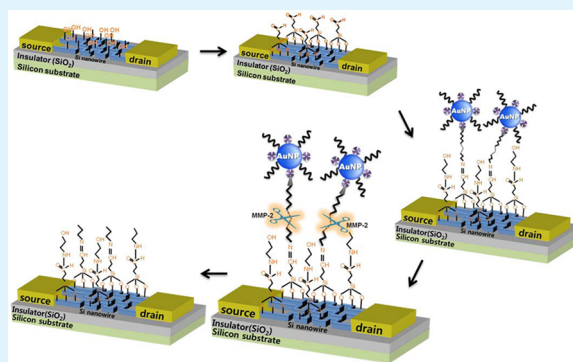
Jin-Ha Choi,<sup>†</sup> Han Kim,<sup>†</sup> Jae-Hak Choi,<sup>‡</sup> Jeong-Woo Choi,<sup>†</sup> and Byung-Keun Oh<sup>\*,†</sup>

<sup>†</sup>Department of Chemical & Biomolecular Engineering, Sogang University, #1 Shinsu-dong, Mapo-gu, Seoul 121-742, Republic of Korea

<sup>‡</sup>Department of Polymer Science and Engineering, Chungnam National University, Yuseong-gu, Daejeon 305-764, Republic of Korea

**ABSTRACT:** Silicon nanowires have been used in the development of ultrasensitive biosensors or chemical sensors, which is originated in its high surface-to-volume ratio and function as field-effect transistor (FET). In this study, we developed an ultrasensitive DNA-gold (Au) nanoparticle complex-modified silicon nanowire field effect transistor (SiNW-FET) biosensor to detect matrix metalloproteinase-2 (MMP-2), which has been of particular interest as protein biomarker because of its relation to several important human diseases, through an enzymatic cleavage reaction of a specific peptide sequence (IPVSLRSG). SiNW patterns with a width of 100 nm and height of 100 nm were fabricated on a p-type silicon-on-insulator (SOI) wafer by electron-beam lithography. Next, negatively charged DNA-Au nanoparticle complexes coupled with the specific peptide (KKGGGGGG-IPVSLRSG-EEEEEE) were applied on the SiNWs to create a more sensitive system, which was then bound to aldehyde-functionalized SiNW. The enhanced negatively charged nanoparticle complexes by attached DNA were used to enhance the conductance change of the p-SiNW by MMP-2 cleavage reaction of the specific peptide. MMP-2 was successfully measured within a range of 100 fM to 10 nM, and the conductance signal of the p-type SiNW by the MMP-2 cleavage reaction was enhanced over 10-fold by using the DNA-Au nanoparticle complexes compared with using SiNW-attached negative single peptide sequences.

**KEYWORDS:** silicon nanowires (SiNWs), nanobiosensor, Au nanoparticle, matrix metalloproteinase-2 (MMP-2), silicon-on-insulator (SOI)



## 1. INTRODUCTION

Protein detection is very important for precise disease diagnosis and early treatment. Proteases, a class of protein biomarkers, have been of particular interest because they are related to several important human diseases, such as cancer and acquired immune deficiency syndrome (AIDS).<sup>1,2</sup> Matrix metalloproteinases (MMP) are very valuable and frequently used protease biomarkers for the study of cancer invasion and metastasis, since they are involved in tumor cell adhesion, extracellular matrix proteolysis, and cell migration.<sup>3–5</sup> In particular, MMP-2 has been used as a biomarker of prostate cancer, breast cancer, and ovarian cancer.<sup>6–9</sup> MMP-2 levels in normal healthy people are lower than in patients with prostatic hyperplasia and prostate cancer.

Common strategies employed for detecting proteins, including MMPs, are enzyme-linked immunosorbent assays (ELISA), which are relatively rapid and simple assays that use antigen–antibody interactions.<sup>10,11</sup> However, they suffer from some disadvantages, including difficulties with sustaining stability, exposing active sites for antigen binding, and the antibody itself easily denaturing with temperature changes.

Especially, it is very difficult to maintain constant activity of the antibody because of its inherent unstable protein properties, which originated in complicated three-dimensional structures. In addition, the sandwich type ELISA system needs two kinds of antibody, a targeting antibody, and a capture antibody. These needs cause not only a complicated process but also required a large quantity of antibodies. Therefore, it is necessary to develop a new protein detection method that does not require the use of antibodies.

Most biosensors include a biological binding event that can be based on an immune reaction for proteins<sup>12–15</sup> and sequence-dependent hybridization for DNA.<sup>16</sup> In contrast, a detachment event through a biological reaction is a good way to detect wanted biomaterials if they disassemble exposed to other specific biomaterials. Fortunately, MMPs are proteolytic enzymes, which play a key role in extracellular matrix degradation, and can be detected through the phenomenon

**Received:** September 5, 2013

**Accepted:** October 28, 2013

**Published:** October 28, 2013

of the detachment of a particular peptide sequence, which is recognized and truncated by MMP.<sup>17</sup> Actually, previously developed MMP assays using unique peptide sequences have already been examined due to the good cleavage ability of the peptides and their potential for use as cancer prognostic markers.<sup>18</sup> This method is superior to immune reaction-based biosensors from a practical standpoint, because it is a nonlabeling method with one-step reaction kinetics, and it does not require the use of unstable and expensive antibodies. Nevertheless, protein assays based on proteolytic cleavage have not been widely used in biosensing applications because of a lack of a suitable analysis system. Most of the specific peptide-relevant MMPs sensing systems are based on fluorescence resonance energy transfer (FRET), a distance-dependent phenomenon between an acceptor and a fluorescent donor.<sup>19</sup> However, a FRET-based sensing system has an inherent photobleaching problem and does not display superior sensitivity when compared with general ELISA.

Silicon nanowire field effect transistors (SiNW-FETs) have recently drawn tremendous attention as a promising tool for biosensors because of their extremely high sensitivity, label-free, and real-time detection capabilities. In particular, they represent suitable systems to evaluate the sensitivity of sensors.<sup>20,21</sup> The ultrahigh sensitive detection ability is attributed to their small size and large surface-to-volume ratio, enabling local charge transfers that result in a current change due to a field-effect when the analytical molecules bind to specific recognition molecules such as an immune reaction on the nanowire surface. Because of these advantages, especially on its sensitivity, SiNW-FETs are an optimal tool for a MMP-2 sensing system based on a specific peptide cleavage reaction.

In previous study, we reported that SiNW-FET based biosensor, which surface is modified with a specific peptide sequence (KKGGGGGG-IPVSLRSG-EEEEEE), for detection of MMP-2 can be used as biosensor for rapid and simple detection of MMP-2 protein without immobilized antibody or any other probes.<sup>22</sup> The SiNW-FET based biosensor exhibit good sensitivity and selectivity for MMP-2. We hypothesized that if the negative surface charge of the *p*-SiNW-FET based biosensor is enhanced with specific functionalities, the sensitivity of the biosensor can be improved drastically. Herein, we demonstrate how one can use a DNA-gold (Au) nanoparticle complex to improve the sensitivity of the SiNW-FET based biosensor with the specific peptide sequence for detection of MMP-2. SiNW patterns were fabricated on a silicon-on-insulator (SOI) wafer using electron-beam lithography. The SOI wafer simplifies the design, as difficulties can arise due to the positioning and reproducibility of the nanowires.<sup>23,24</sup> Furthermore, a negatively charged Au nanoparticle complex coupled with a specific peptide was applied to the SiNW-FET in order to create a more sensitive system. Typically, using Au nanoparticles with other biomaterials has been shown to enhance the sensitivity of the detection signal due to the nanoparticles' small size, optical and electrical properties, and silver stained property.<sup>25–27</sup> In this system, Au nanoparticles had their negative charges enhanced by attaching thiolated-DNA strands, which are characterized by their negatively charged phosphate backbones. The increased negative charge of the attached materials improves the sensitivity of the SiNW-FET. This hybrid system composed of Au nanoparticles, SiNW-FET, and other biomaterials showed effective sensing abilities, particularly effective for

ultrasensitive detection of MMP-2, with concentrations as low as 100 fM.

## 2. MATERIALS AND METHODS

**2.1. Materials.** *p*-Type silicon-on-insulator (SOI) wafers (insulating layer, 145 nm; silicon layer, 55 nm) were purchased from Soitec Co. (France). 3-(triethoxysilyl)butylaldehyde (TESBA) was purchased from Gelest, Inc. (USA). Distilled and deionized Millipore water (Milli-Q) and N<sub>2</sub> gas were used for cleaning and drying. The designed peptide (KKGGGGGG-IPVSLRSG-EEEEEE-biotin) was synthesized by Peptron Inc. (Korea). The designed thiol-modified DNA fragment (SH-AGAGAGAGAGAGAGAGAGAG) was synthesized by Genotech Inc. (Korea). Polyethylene glycol functionalized amine group (NH<sub>2</sub>-PEG) and phosphate buffered saline (PBS) purchased from Sigma Aldrich Inc. (Germany). Au nanoparticles with a diameter of 60 nm were purchased from BBInternational (Cardiff, UK).

**2.2. Fabrication of the Peptide-Attached Au Nanoparticle Complex.** To prepare the Au nanoparticles, 1 mL of an aqueous suspension of colloidal Au nanoparticles (60 nm,  $2.6 \times 10^{10}$  per mL) was centrifuged for 5 min at 10,000 rpm, and the supernatant was removed. The particles were resuspended in a 0.01 M PBS solution at pH 7.4, and 1 mg/mL of streptavidin was added to the solution and incubated for 2 h to immobilize the biotinylated peptide. Then, 1 mg/mL of a 5' thiolated DNA fragment was added to the solution to bind on the AuNP surface through an Au-thiol interaction. The solution was incubated on a rocking shaker for 2 h at room temperature, centrifuged for 10 min at 10 000 rpm, and the supernatant was removed to eliminate free streptavidin and DNA fragments. This washing step was repeated several times until the residues were completely removed. Designed biotinylated peptides (KKGGGGGG-IPVSLRSG-EEEEEE-biotin) were then added to the nanoparticle solution and incubated on a rocking shaker for 30 min at 4 °C. After several washing steps in PBS (0.01M, 0.05% Tween20, pH7.4), the UV spectrum of the bare Au nanoparticle, attached streptavidin, DNA, and peptide were measured to confirm binding of each biomaterial to the Au nanoparticle surfaces based on the red-shift of the absorbance peak.

**2.3. SOI Nanowire Device Fabrication.** SiNWs on the SOI wafer were designed to have a square-wave formation, which was used to increase the surface area. Electron-beam lithography was then used to construct the SiNWs presented in.<sup>22</sup> A square-wave pattern was placed on the top silicon area (nanochannel width: 100 nm ; total length: 40 μm) and the unneeded silicon area was removed by etching. The square-wave pattern consisted of 25 nanowires with a width of 100 nm and height of 100 nm. All electrical properties of the SiNWs on the SOI substrate were measured using a B1500A semiconductor parameter analyzer system (Keithley Co., USA). The nanowire structures on the SOI substrate were characterized using scanning electron microscopy (SEM, JSM-6700, 15–30 kV).

**2.4. Fabrication of the Au Nanoparticle Complex Functionalized SiNW Patterns.** Fabricated nanowire patterns were cleaned with an O<sub>2</sub> plasma at 50 W for 60 s. The nanowire-patterned chips were then immersed in a TESBA (3-(triethoxysilyl)butylaldehyde) solution (1% v/v in ethanol/H<sub>2</sub>O (95%/5%)) for 30 min at room temperature to allow for the formation of self-assembled monolayers (SAMs) and washed with absolute ethanol several times. These functionalized nanopatterns were incubated in a solution of assembled Au nanoparticle complexes (DNA-Au-streptavidin-peptide) in a PBS buffer for 2 h at room temperature to allow for binding between the Au nanoparticle complexes and SiNW surface through an aldehyde-amine interaction. After 2 h, the Au nanoparticle complexes were immobilized on the nanowire patterns, which were then rinsed with deionized water and PBS buffer, and dried with N<sub>2</sub> gas several times. Afterward, the nanowire patterns were incubated in a solution of 1 mg/mL NH<sub>2</sub>-PEG in PBS buffer to block nonspecific binding to the SiNW surface. Finally, MMP-2 concentrations ranging from 100 fM to 10 nM were applied to the system

### 3. RESULTS AND DISCUSSION

#### 3.1. Characterization of Au Nanoparticle Complex.

The Au nanoparticle (60 nm) complex consisting of streptavidin, thiolated DNA and a biotin-peptide fragment is shown in Figure 1A. This structure was designed to increase the

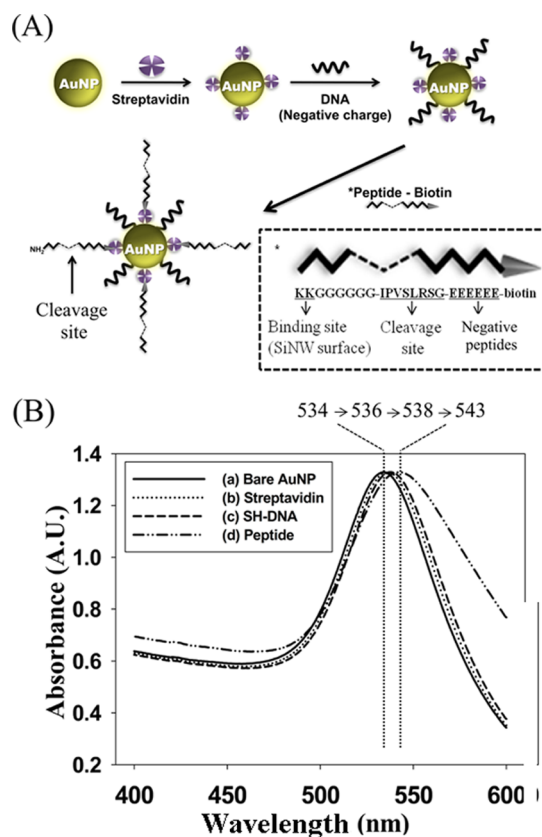


**Figure 1.** (A) Schematic diagram of the Au nanoparticle complex consisting of streptavidin, DNA, and biotinylated peptide. (B) UV-vis spectrum of AuNPs, streptavidin, DNA, and peptide, confirming the adhesion of several biomaterials to the Au nanoparticle. Au nanoparticle had a sharp absorbance peak at 534 nm that red-shifted after the reactions ((a) bare Au nanoparticle; (b) streptavidin 536 nm; (c) DNA 538 nm; (d) peptide 543 nm).

sensitivity and recognition of the target molecule, MMP-2. To increase the sensitivity of the SiNW-FET system, it is essential to give negative charge to the Au nanoparticles so that their removal from the SiNW surface will result in a more drastic and observable decline in current in the case of a *p*-type SiNW-FET. Thiolated DNA is a good biomaterial to impart a negative charge to the Au nanoparticle complex due to the intrinsic negative charge of DNA and ease of surface modification through Au-S bonding. The specificity of this sensing system was characterized by designing a unique peptide sequence reacted with proteolytic proteins, MMP-2. It displays enzymatic activity for the specific peptide IPVSLRSG, which it recognizes and cleaves. This peptide attached to the Au surface based on the interaction between streptavidin and biotinylated peptides. In this way, the nanoparticle can exhibit specific reactive properties when attached to a peptide containing the IPVSLRSG sequence.

The conformation of the Au nanoparticle complex was confirmed based on the UV/vis absorbance spectrum. Figure 1B shows the UV/vis absorbance spectrum of each nanoma-

terial (bare Au nanoparticle, streptavidin, thiolated DNA, and peptide). Au nanoparticles had a single absorbance peak at about 530 nm, which was shifted to the right (red) after biomaterials were attached to their surface due to the LSPR (localized surface plasmon resonance) effect.<sup>28,29</sup> The red-shift of the absorption spectra for the Au nanoparticle depended on nanoparticle size, aggregation, and the local dielectric environments of the attached biomaterial. This absorbance method was suitable for directly identifying binding events between biomaterials and nanoparticles. As shown in Figure 1B, the absorbance peak of the AuNPs was at 534 nm and the peak for the AuNPs complex was shifted to the right when biomaterials were added (Streptavidin 536 nm; DNA 538 nm; peptide 543 nm). Therefore, adhesion of the biomaterials to the Au nanoparticle was demonstrated by the red-shifted absorbance peak.

**3.2. Fabrication of SiNW Device.** The structure of the SOI wafer contained three layers: a substrate Si wafer, a buried silicon dioxide (375 nm thick), and a top Si layer (100 nm thick). Through standard photolithography procedures, reactive ion etching, ion implantation, electron-beam width of the SiNWs reached a scale of about 100 nm. Electron-beam lithography has the advantages of being a standard semiconductor technique that is used to precisely design a device-array pattern without the problems associated with positioning the SiNWs. As shown in panels A and B in Figure 2, SiNWs were successfully and uniformly fabricated on the SOI substrate in a square-wave structure. This structure is superior to the linear form nanowires for biosensing applications due to the wider reactive surfaces. Compared to a linear structure of the same area, this structure has twice the reactive surface area, which is expected to improve the sensitivity of the reaction.

The electrical properties of the device arise from the charge transfer through the SiNW, where the voltage is applied to the input terminal and can be used to control the output current. The current flow through the SiNW between the source and the drain can be controlled by the applied gate voltage. A slight change in the gate voltage can cause a large change in the current flow from the source to the drain. In the case of *p*-type SiNWs, applying a negative gate voltage results in an increase in current flow, which causes an accumulation of electrons. On the other hand, applying a positive gate voltage decreases the conductance since it depletes the electrons. The electrical property of the fabricated *p*-type SiNW devices were assessed using the B1500A semiconductor device analyzer (Agilent Technologies.co, USA) and the SiNW-FET device operated as expected. In Figure 2D, it is clearly shown that when a negative gate voltage is applied, the amount of current that flows through the *p*-type SiNW increases because of the accumulation of electrons.

**3.3. Detection of the MMP-2 with Enhanced Electrical Signal.** For the purpose of detecting MMP-2, it is essential to functionalize the SiNW surface for Au nanoparticle complexes with respect to the constituent parts: the cleaved peptide sequence and the negatively charged nanomaterial (Figure 3). Bare SiNWs were functionalized with a hydroxyl group using O<sub>2</sub> gas plasma treatment and then a chemical linker, TESBA, was attached using the self-assembled monolayers (SAMs) technique. The headgroup of the TESBA reacts with the hydroxyl groups on the SiNW surface to form a tripod shape, through which the tail group can become anchored to the amine-functionalized biomaterials. Because all the peptides contained an amine group on the N-terminal, these modified

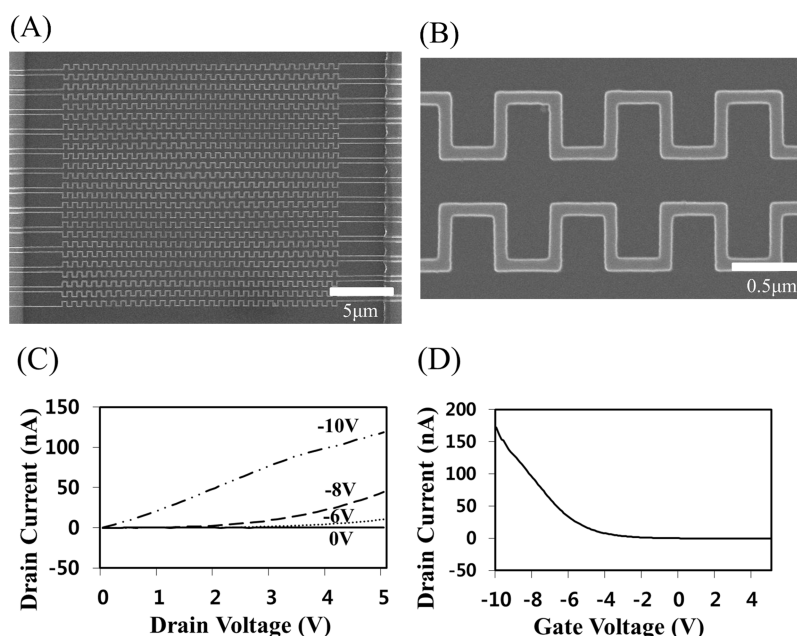


**Figure 2.** Structural shape and electrical properties of the SiNWs. SEM image of the fabricated SiNW patterns, where a square-wave structure was used on a SOI wafer using electron-beam lithography scaled at (A) 10 and (B) 1  $\mu\text{m}$ . (C) Source–drain current ( $I_{\text{sd}}$ ) vs source–drain voltage ( $V_{\text{sd}}$ ) plots at different gate voltages for a typical device in the array. The curves correspond to  $V_{\text{g}}$  values of  $-10$ ,  $-8$ ,  $-6$ , and  $0$  V, respectively. (D)  $I_{\text{sd}}$  vs gate voltage ( $V_{\text{g}}$ ) recorded for a typical device plotted with a  $V_{\text{sd}}$  of 10 V.

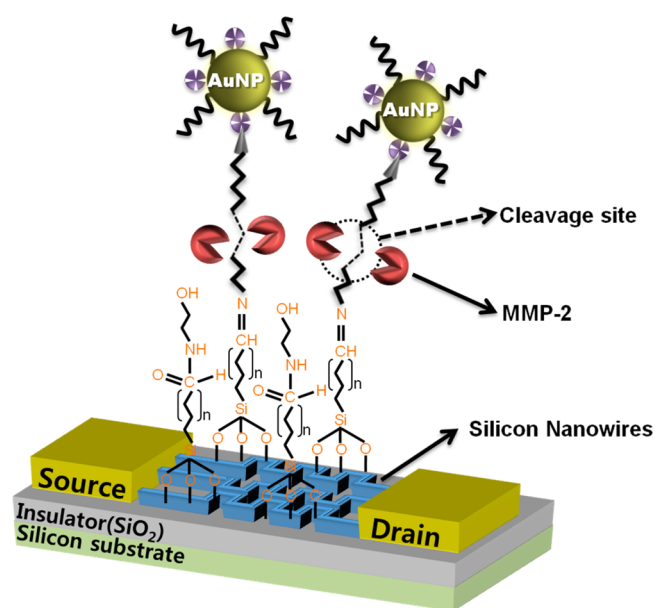


**Figure 3.** Schematic of the SiNW-FET biosensor, based on Au nanoparticle complexes on SiNWs. The peptide contains an amine residue that is used to conjugate the peptide sequence to the SiNW surface, six glutamic acid residues to impede electric current, MMP-2 cleavage site (IPVSLRSG), and biotinylated c-terminal. MMP-2 cleaved the specific peptide sequence (IPVSLRSG), resulting in a change in the conductance.

peptide fragments were able to attach to the aldehyde-functionalized SiNW surface. As shown in Figure 3, the artificial peptide-modified Au nanoparticle complexes were attached to the SiNW surface in order to detect MMP-2. The Au nanoparticle complexes play a crucial role in the SiNW-FET biosensor, by increasing the sensitivity through a higher conductance value, which amplifies the decreasing conductance

signal when MMP-2 is applied to the device. After immobilization of the Au nanoparticle complexes,  $\text{NH}_2$ -PEG was applied to the device at a concentration of 1 mg/mL. The major role of PEG is to block other reactions, such as any interaction between MMP-2 and the SiNW surface, which contain hydroxyl and aldehyde groups. As a result, this defensive step prevents inaccurate signal generation.

As mentioned above, Au nanoparticle complexes can be placed on the SiNW surface in order to improve the sensitivity of this sensor. In the case of p-type SiNW-FET, a decrease in the current will be expected when negative charges are removed from the sensing surface. That is why attachment of a negatively charged Au nanoparticle complex is a critical factor in this sensing system with the intent to increase the sensitivity to MMP-2. In practice, a six-glutamic acid residue group was used in the designed peptide (KKGGGGGG-IPVSLRSG-EEEEEE), characterized by negative charge because of its acidity in neutral conditions, which assists in increasing electric current with respect to the bare SiNW surface.

Moreover, DNA-functionalized Au nanoparticle complexes are highly negatively charged due to the presence of the phosphate ion in its backbone. For that reason, negatively charged Au nanoparticle complexes are essential for ultra-sensitive MMP-2 detection. The enhanced signal generation resulting from the use of the Au nanoparticle complexes is shown in Figure 4. The difference in conductivity was much greater when the DNA-Au nanoparticle complexes were used relative to the use of just the peptide. The sensing signal exhibited 14-fold and 12-fold enhancements for MMP-2 concentrations of 10 and 1 nM, respectively. That is, remarkably, the 1 nM MMP-2 signal using the Au nanoparticle complex is greater than the signal obtained when injecting 10 nM MMP-2 and using only the peptide sequence. These results clearly show that the use of the Au nanoparticle complex enhances signal generation by at least 10-fold relative to the use of the peptide alone.

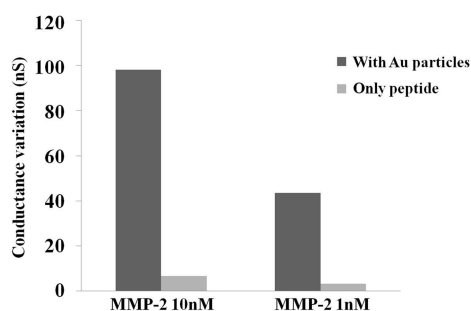


**Figure 4.** Conductance change when using the Au nanoparticle complex or the peptide alone. MMP-2 concentrations were 10 and 1 nM.

To apply protein sensing system, MMP-2 was supplied to the device at concentrations ranging from 100 fM to 10 nM. As shown in Figure 5A, the magnitude of the conductance changes

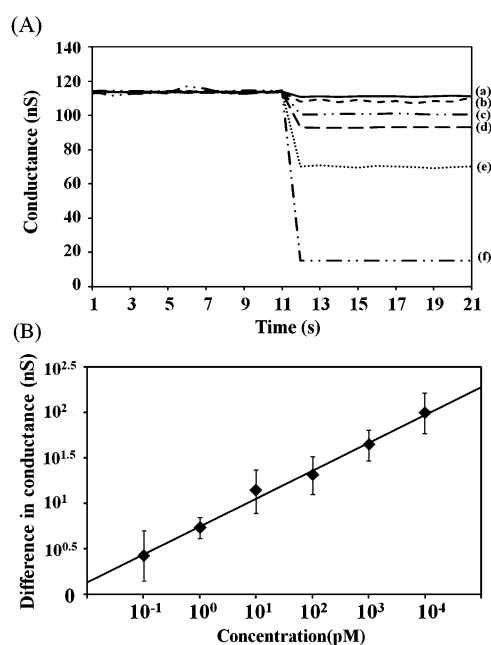


**Figure 5.** Difference in conductance after delivery of MMP-2 using DNA-Au nanoparticle complexes. (A) Conductance vs time data measured after alternate delivery of MMP-2 correspond to concentrations of (a) 100 fM, (b) 1 pM, (c) 10 pM, (d) 100 pM, (e) 1 nM, (f) 10 nM. (B) Log [Conductance variation] as a function of concentration.

was dependent on MMP-2's cleavage reaction with the specific peptide sequence at the surface of the p-type SiNW. The decrease in current resulted from a cleavage reaction between the target peptide sequence (IPVSLRSG) and MMP-2; this was shown to have a significant effect on the surface conductivity of the SiNW-FET. After MMP-2 interacted with the specific peptide sequence, the conductance and current decreased and the Au nanoparticle complexes were cleaved from the SiNW surface.

The lowest detectable concentration and detection range of MMP-2 using the Au nanoparticle complexes modified SiNW-FET is shown in Figure 5B. Concentration-dependent electric responses were observed for MMP-2 at concentrations ranging from 100 fM to 10 nM. Moreover, the time required for the conductance change was approximately 13 s and the negative

control signal showed almost no conductance variation with 2.5 signal-to-noise ratio in case 0.1 pM concentration. This result strongly suggests that a rapid and sensitive sensing device for the detection of MMP-2 was achieved.

#### 4. CONCLUSION

In this study, we successfully developed signal enhancing MMP-2 biosensor using a SiNW-FET device that was fabricated using electron-beam lithography using negative Au nanoparticle complexes. Using the fabricated SiNW-FET device, different concentrations of MMP-2 were sequentially measured in terms of conductance versus time at MMP-2 concentrations ranging from 100 fM to 10 nM. The use of the Au nanoparticle complex was shown to improve the sensitivity by 10-fold relative to the peptide alone. This result is the most sensitive MMP-2 detectable sensor published to date. The developed SiNW-FET sensor possesses several advantages, such as good analytical performance, clear conductance response and high sensitivity, low detection limits within an appropriate linear range. In addition, this SiNW-FET sensor could be mass produced at low cost if another etching method, such as nanoimprint lithography, was used. Taken together, the results of this study make it clear that the proposed system holds great promise for use in ultrasensitive biosensing and electroanalytical applications.

#### AUTHOR INFORMATION

##### Corresponding Author

\*E-mail: bkoh@sogang.ac.kr.

##### Author Contributions

The manuscript was written through contributions of all authors. All authors have given approval to the final version of the manuscript.

##### Notes

The authors declare no competing financial interest.

#### ACKNOWLEDGMENTS

This research was supported by the Original Technology Research Program for Brain Science through the National Research Foundation of Korea(NRF) funded by the Ministry of Education, Science and Technology (2012-0006592) and radiation Technology R&D program through the National Research Foundation funded by the Ministry of Science, ICT & Future Planning, Korea and by the Human Resources Development of the Korea Institute of Energy Technology Evaluation and Planning(KETEP) grant funded by the Korea government Ministry of Knowledge Economy (20114010203090)

#### ABBREVIATIONS

- FET, field effect transistor
- Au, gold
- SiNW, silicon nanowire
- MMP, matrix metalloproteinase
- SOI, silicon-on-insulator
- ELISA, enzyme-linked immunosorbent assays
- FRET, fluorescence resonance energy transfer
- TESBA, 3-(triethoxysilyl)butylaldehyde
- PEG, polyethylene glycol
- AuNP, gold nanoparticle
- SAM, self-assembled monolayer

## ■ REFERENCES

- (1) Zolnierowicz, S.; Bollen, M. *Embo J.* **2000**, *19*, 483–488.
- (2) Shults, M. D.; Janes, K. A.; Lauffenburger, D. A.; Imperiali, B. *Nat. Methods* **2005**, *2*, 277–284.
- (3) Pia, V.; Veli-Matti, K. *Int. J. Cancer.* **2002**, *99*, 157–166.
- (4) Chambers, A. F.; Matrisian, L. M. *J. Natl. Cancer Inst.* **1997**, *89*, 1260–1270.
- (5) Duffy, M. J.; McCarthy, K. *Int. J. Oncol.* **1998**, *12*, 1343–1348.
- (6) Giuseppe, M.; Mario, F.; Grazia, M.; Massimo, M.; Manuela, I.; Salvatore, T.; Maria, C. M. *Urol. Res.* **2005**, *33*, 44–50.
- (7) Gershenwald, J. E.; Sumner, W.; Calderone, T.; Wang, Z.; Huang, S.; Bar-Eli, M. *Oncogene* **2001**, *20*, 3363–75.
- (8) Tan, M.; Yao, J.; Yu, D. *Cancer Res.* **1997**, *57*, 1199–205.
- (9) Ayla, A.; Onan, A.; Coskun, U.; Uner, A.; Bagriacik, U.; Atalay, F.; Unsal, D. K.; Guner, H. *Med. Oncol.* **2008**, *25*, 279–283.
- (10) Yates, A. M.; Elvin, S. J.; Williamson, D. E. *J. Immunoassay* **1999**, *20*, 31–44.
- (11) Barascuk, N.; Veidal, S. S.; Larsen, L.; Larsen, D. V.; Larsen, M. R.; Wang, J.; Zheng, Q.; Xing, R.; Cao, Y.; Rasmussen, L. M.; Karsdal, M. A. *Clinbiochem.* **2010**, *43*, 899–904.
- (12) Cheng, I. F.; Yang, H. L.; Chung, C. C.; Chang, H. C. *Analyst* **2013**, *138*, 4656–4662.
- (13) Zhang, J.; Sun, Y.; Xu, B.; Zhang, H.; Gao, Y.; Zhang, H.; Song, D. *Biosens. Bioelectron.* **2013**, *45*, 230–236.
- (14) Wang, J.; Yau, S. T. *Electrochim. Acta* **2013**, *111*, 92–98.
- (15) Kang, D. Y.; Lee, J. H.; Oh, B. K.; Choi, J. W. *Biosens. Bioelectron.* **2009**, *24*, 1431–1436.
- (16) Luo, C.; Tang, H.; Cheng, W.; Yan, L.; Zhang, D.; Ju, H.; Ding, S. *Biosens. Bioelectron.* **2013**, *48*, 132–137.
- (17) Leight, J. L.; Alge, D. L.; Maier, A. J.; Anseth, K. S. *Biomaterials* **2013**, *30*, 7344–7352.
- (18) Kim, Y. P.; Oh, Y. H.; Oh, E.; Ko, S.; Han, M. K.; Kim, H. S. *Anal. Chem.* **2008**, *80*, 4634–4641.
- (19) Achatz, D. E.; Mezo, G.; Kele, P.; Wolfbeis, O. S. *ChemBiochem.* **2009**, *10*, 2316–2320.
- (20) Choi, D. S.; Lee, J. H.; Jung, H. S.; Jung, G. Y.; Choi, J. H.; Choi, J. W.; Oh, B. K. *J. Nanosci. Nanotechnol.* **2011**, *11*, 4517–4521.
- (21) Kim, H.; Lee, J. H.; Chae, E. J.; Choi, J. W.; Oh, B. K. *J. Nanosci. Nanotechnol.* **2011**, *11*, 7516–7519.
- (22) Choi, J. H.; Kim, H.; Kim, H. S.; Um, S. H.; Choi, J. W.; Oh, B. K. *J. Biomed. Nanotechnol.* **2013**, *9*, 291–294.
- (23) Cui, Y.; Duan, X.; Hu, J.; Lieber, C. M. *J. Phys. Chem. B.* **2000**, *104*, 5213–5216.
- (24) Duan, X.; Huang, Y.; Cui, Y.; Wang, J.; Lieber, C. M. *Nature* **2001**, *409*, 66–69.
- (25) Gittins, D. I.; Bethell, D.; Schiffrin, D. J.; Nichols, R. J. *Nature* **2000**, *408*, 67–69.
- (26) Lee, W.; Oh, B. K.; Kim, Y. W.; Choi, J. W. *J. Nanosci. Nanotechnol.* **2006**, *6*, 3521–3525.
- (27) Choi, J. W.; Oh, B. K.; Jang, Y. H.; Kang, D. Y. *Appl. Phys. Lett.* **2008**, *93*, 033110.
- (28) Delfino, I.; Cannistraro, S. *Biophys. Chem.* **2009**, *139*, 1–7.
- (29) Li, L.; Mu, Q.; Zhang, B.; Yan, B. *Analyst* **2010**, *135*, 1519–1530.